Available online at www.sciencedirect.com

ScienceDirect

Procedia CIRP 85 (2019) 96–101

www.elsevier.com/locate/procedia

2nd CIRP Conference on Composite Material Parts Manufacturing (CIRP-CCMPM 2019)

# Numerical and Experimental Investigation of Thermoplastics in Multi-Axis Forming Processes

Klaus Dröder[b], Bernd-Arno Behrens[a], Florian Bohne[a], Alexander Chugreev[a], Henrik Schulze[a], Birk Wonnenberg[b]*

[a] *Institute of Forming Technology and Machines, Leibniz Universität Hannover, An der Universität 2, 30823 Garbsen, Germany*
[b] *Technische Universität Braunschweig, Institute of Machine Tools and Production Technology, Langer Kamp 19b, 38106 Braunschweig, Germany*

* Corresponding author. Tel.: +49-531-391-7178; fax: +49-531-391-5842. *E-mail address:* b.wonnenberg@tu-braunschweig.de

**Abstract**

Process planning for multi-axis forming presses is a particular challenge. This process provides the option to actively influencing the material flow in the forming process by defining a six dimensional tool motion path and the tool velocity. By comprehending this interaction, it is possible to control and thereby tailor the induced local material properties of the workpiece. Experiments were conducted with a multi-axis press, which is based on a Stewart platform. A simple plane workpiece geometry is chosen to analyse the flow behaviour and the temperature evolution of the glass mat thermoplastics (GMT) during the forming process. Subsequently, a numerical simulation of the multi-axis forming process is carried out and validated with the experimental data. The numerical analysis focuses on the material modelling as well as the prediction of the flow characteristics. Regarding material modelling of GMT, an extensive material characterization is performed to describe the flow behaviour. A prediction of the flow behaviour of GMT with reference to tool motion is enabled. For the FE simulation the element-free Galerkin method (EFG) is applied for modelling the fluid structure interaction and adaptive procedures.

© 2020 The Authors. Published by Elsevier B.V.
This is an open access article under the CC BY-NC-ND license (http://creativecommons.org/licenses/by-nc-nd/4.0/)
Peer-review under responsibility of the scientific committee of the 2nd CIRP Conference on Composite Material Parts Manufacturing.

Keywords: Forming; Fiber reinforced plastic; Temperature; Kinematic; Finite element methode (FEM)

## 1. Introduction

Fibre reinforced plastics (FRP) are commonly used to integrate multiple parts into one complex component and reduce part weight by substituting pure metal parts. FRP materials base on a polymeric matrix and fibre reinforcement. Commonly applied fibre materials are carbon, glass and natural fibres and are typically available as short, long or endless fibres. For the design process of one specific global material and part behaviour numerical simulations are conducted in order to analyse and optimise the forming process. To simulate FRP materials the mechanical properties of fibre and matrix material in the process need to be known. The flow behaviour is strongly temperature dependent and hence sets high requirements for the process. All interactions and influences must be considered for a reliable description of the forming behaviour and therefore the mechanical part behaviour.

The research presented in this paper refers to the application of glass mat reinforced thermoplastic composite (GMT) material, which is based on randomly aligned glass fibres and polyamide 6. A multi-axis forming process is investigated in this research. Besides one axis in common pressing processes, further additional axes are used to realise a tool motion to induce a specific material flow. The flow pattern can be defined for example in the part design beforehand in order to align the glass fibres.

With the alignment of the glass fibres through the pressing process anisotropic material behaviour can be obtained [1]. The intentionally induced anisotropy can be used to enable advantageous mechanical properties in the context of lightweight design. Furthermore, multi-axis forming can be applied in order to manufacture highly complex hybrid components of FRP and metal, which seems to be a promising approach for an efficient lightweight production [2, 3]. The process can reduce misalignment of inserts and minimise

2212-8271 © 2020 The Authors. Published by Elsevier B.V.
This is an open access article under the CC BY-NC-ND license (http://creativecommons.org/licenses/by-nc-nd/4.0/)
Peer-review under responsibility of the scientific committee of the 2nd CIRP Conference on Composite Material Parts Manufacturing.
10.1016/j.procir.2019.09.024

This is a resupply of March 2023 as the template used in the publication of the original article contained errors. The content of the article has remained unaffected.

porosity within the boundary zone of adjacent materials through induced material flow. In the scope of the here presented work, a numerical simulation is carried out in order to predict the material flow. Subsequently, the numerical results are compared to the experiments. Finally, conclusions of the presented work are drawn.

## 2. Material characterisation

For composite materials there are several combinations regarding fibre type, orientation, composition and polymer material. Already in the design stage, the composite material is specified with regard to the forming process. With reference to the great number of FRP combinations, the material differs in its properties, e.g. flow behaviour. For a few composite materials rheometric tests can be used to describe the mechanical behaviour. Different scientific work exists for the characterisation of the flow behaviour for GMT material. Squeeze flow testing is the primarily applied parametrisation method [4, 5]. Several approaches for deriving material model parameters from squeeze flow data are presented in [6].

The primary chosen approach in literature for modelling the flow behaviour of GMT is the description as a non-Newtonian fluid. Herein, the flow behaviour is described with help of the viscosity, which itself is described depending on the flow regimes. During tool closure extensional flow as well as shear flow can be observed [7]. Both can be described with help of a power law model [8], which takes into account the influences of shear rate, strain rate and strain hardening effects [5]. In the context of continuums mechanics, a generalised Newtonian fluid with a degenerating viscosity can be described through an idealised plastic material model [6]. This approach makes it possible to derive a plastic material model based on the viscosity data [9].

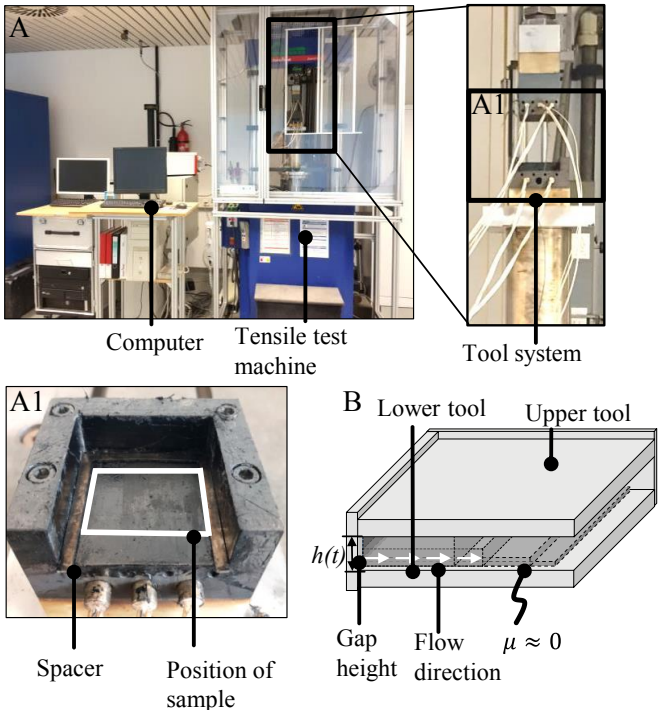


Fig. 1. Experimental press rheometry set up and sketch of material flow ($\mu$-coefficient of friction)

In order to ensure accurate input data for the flow behaviour of the used material, an experimental set up has been created and press rheometry tests have been carried out for the applied GMT material. Fig. 1 shows the experimental set up (A, A1) and the expected flow behaviour in the press gap (B). After heating to a homogenous temperature the specimens are pressed with a velocity of 0.5 mm/s. The spacer limits the minimum gap height to 2 mm. An anti-sticking foil is inserted in order to reduce friction. In Fig. 2 the measured force is plotted over the gap height. In order to exploit the sophisticated plastic material model formulations in LS-DYNA, a flow curve is derived from the experimental data for each test temperature. The measured forces over height and the derived flow curves are plotted in Fig. 2. For the temperature range from 230 °C up to 290 °C the force as well as flow stress curves show identical characteristics regarding the curve shape. The measured forces at a test temperature of 230 °C are higher due to the increasing matrix stiffness, caused by the proximity to the solidification temperature (219°C). Additionally, an increase in force is observed in a gap height range from 2.5 mm to 2.0 mm for all temperatures. This is caused by the compaction of the fibre bed. An averaged flowcurve over the investigated test temperatures is computed (Fig. 2 right, blue curve).

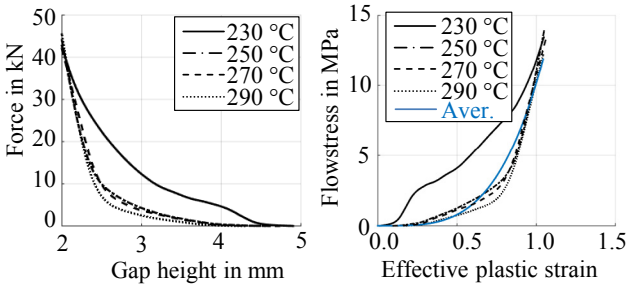


Fig. 2. Force over gap height (left) and derived flow curves (right)

## 3. Experimental characterization of the multi-axis forming process

For the experiments a forming press with parallel kinematic was used. This kinematic is based on a hydraulic actuated Stewart platform, which can move the upper tool in all six axes. The machine was intentionally built to reduce the mechanical complexity of orbital forming [10]. The machine with a forming tool and forming material are displayed in Fig. 3. The workspace of this machine is designed cylindrical with a height of 50 mm (z-axis) and a diameter of 100 mm (x- and y-axis). In this workspace, the upper tool can be rotated by 5 ° around the vertical axis (C-rotation-axis) and by 15 ° around the other axis (A- and B-rotation-axis). For the forming process, the machine applies a force up to 50 kN in z-axis and 5 kN in x- and y-axis.

For the experiments, a plain lower die and a curved upper tool were used. With these tools, the forming material is pressed to a plate with a rolling movement of the upper tool. The lower tool is equipped with thermocouples on the surface to measure the surface temperature of the compound in the forming process.

This is a resupply of March 2023 as the template used in the publication of the original article contained errors. The content of the article has remained unaffected.

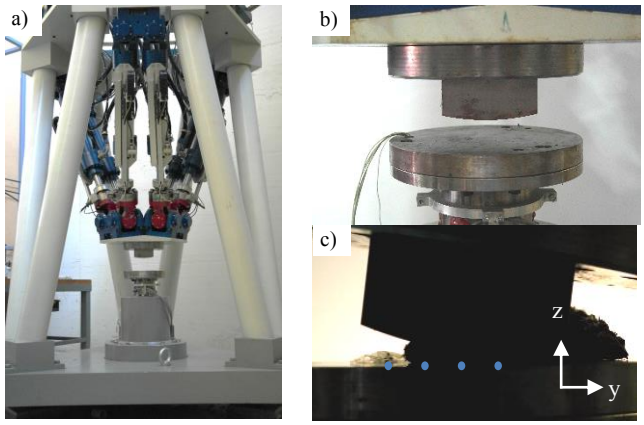


Fig. 3. a) image of the experimental machine; upper part: six hydraulic actors with glass scales and load cells; b) upper and lower tool; c) position of the thermocouples in the process

The process is subdivided into three phases: Heating of the forming material in an oven, insertion of the material into the press and the pressing and rolling phase. The material was melted in a convection oven for 20 min. at 260 °C and inserted into the press after the matrix was molten. It is placed on one side of the lower tool and pressed to the other side in three forming steps. The tilted upper tool is moved at a velocity of 30 mm/s along the vertical movement (z-axis) to the starting position of the rolling movement. With this movement, the compound is pressed between the resulting nip. In the next forming step, the material is formed with a rolling movement of the upper tool. The upper tool rotates (A-rotation axis) around the tool centre point without a relative movement to the resulting part surface. After rolling, the upper tool moves along z-axis to end the forming process. The motion path of the tool centre point at the tip of the upper tool is displayed in Fig. 4.

The tool motion in tests 3 and 5 is defined by two positions (start and end position) which are connected by linear interpolation. With this motion the height of the resulting plate is formed. Tests 1, 2 and 4 have an additional third position in the middle of the forming process with a short resting time in the forming process to obtain a reference point in the material flow. This reference point can be used to synchronize the measurements afterwards as well as to compensated possible deviations in the forming movement, which can occur in a multi-axis forming process without spacers.

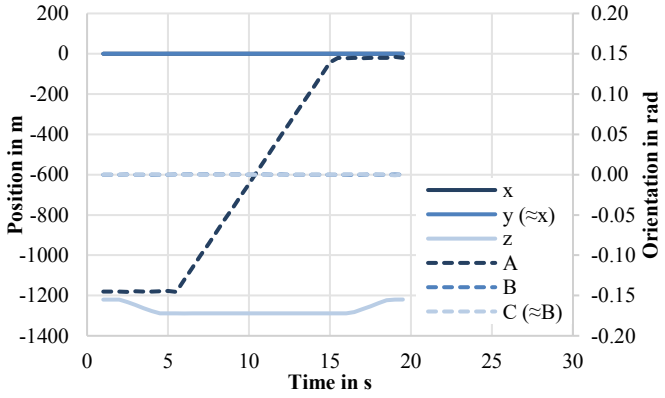


Fig. 4. Upper tool motion in the forming process

To compare the experiments to the simulation results, the process was observed sideways in an open tool setup. A camera captures the tool movement and the material position and shape. With this information, the expanse of the flow front can be calculated. An image processing algorithm searches for the furthest extend of the forming material in the image. The positon of this flow front is measured relatively to the forming tool in the image. The results from the image processing and the forming material, coloured in blue, are displayed in Fig. 5. The farthest left (1) and right (2) flow front are marked with a dashed line.

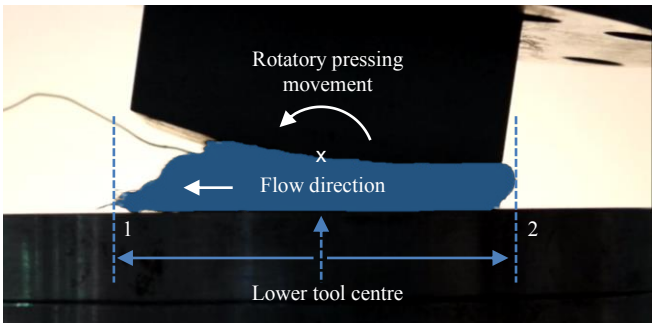


Fig. 5. Forming process of the molten GMT in an open die with an over layer of the image processing colouring the compound in blue; the farthest left and right edge of the compound are marked (1, 2) and the distance to the tool middle is determined

The results of the image processing and the temperatures from the forming experiments are presented in the following section. The results focus on the left flow front in these experiments, which are measured optically. All measurements are synchronised afterwards by setting the first steep rise of the signal as fifth second of process time. After this, the forming process takes another 15 s.

Five tests were conducted and altered by the insertion point of the forming material. In addition, the shape of the material varies. The material cannot be kept in a certain shape after heating because of the tacky surface and high porosity. The position and shape of the compound are approximated by using an ellipse. The parameters of this shape can be determined by drawing the smallest ellipse including every apart of the inserted material and the biggest ellipse including only the inserted material. The averages of theses parameters were calculated and displayed for each test in Table 1. In addition, the percentages of the area of the ellipses under the punch were determined. The ellipses are also displayed in Fig. 6.

Table 1: Initial position of the compound approximated by an ellipse in mm; x and z are the position of the ellipse middle to the tool middle; a and b are semi-major and semi-minor axis; percentage of the area of the ellipse under the upper tool before pressing

| Test | x | z | a | b | Percentage under the punch |
|---|---|---|---|---|---|
| 1 | 45 | 13 | 60 | 18 | 0.58 |
| 2 | 38 | 14 | 61 | 17 | 0.63 |
| 3 | 34 | 15 | 58 | 21 | 0.65 |
| 4 | 27 | 25 | 58 | 28 | 0.70 |
| 5 | 10 | 14 | 61 | 19 | 0.81 |

This is a resupply of March 2023 as the template used in the publication of the original article contained errors. The content of the article has remained unaffected.

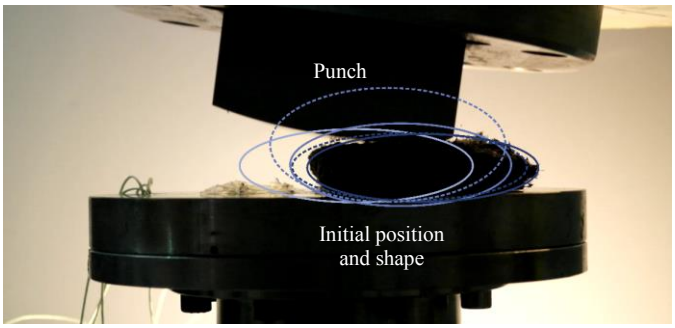


Fig. 6. Insert position and shape of the compound approximated by an ellipse, dark blue line test 1, dark blue dotted line test 2, blue line test 3, blue dotted line test 4 and light blue line test 5

In Fig. 7, the progress of the left flow front in the forming process is displayed. The flow front proceeds rapidly while the upper tool moves along z-axis and slower to the maximum expanse, while the tool rotates over the surface. Test 1, 2 and 4 show a small peak at 12 s. This peak correlates with the extra point in the path description for the upper tool movement. The initial position of the flow front, values under 5 s, correlates to the initial position of the material.

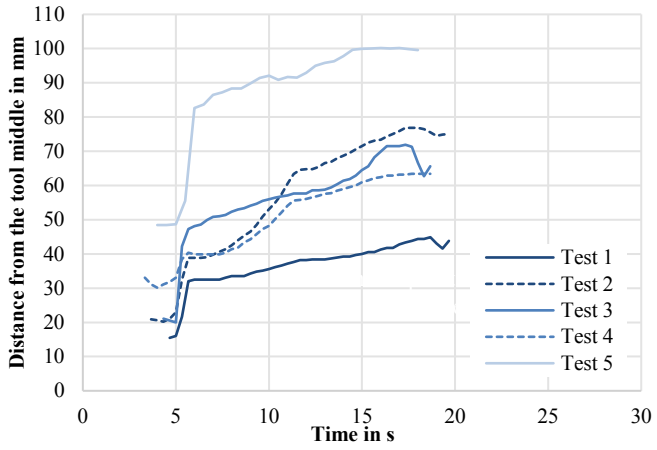


Fig. 7. Movement of the flow front to the left side measured optically from the centre of the lower tool

The temperatures in the process were measured in the boundary layer for all five tests and displayed for all four sensors (see positions in Fig. 3). In Fig. 8, the temperature for at theses sensors in each test are displayed and test 3 (c) is exemplary described. The other tests show a comparable qualitative progression to each other.

The surface temperature of the compound reaches the lowest peak value for the insertion position, here sensor 1 and 2. In the progress, the compound contacts the other sensors. These sensors reach higher peak values than the first two. Sensor 4 is not always in contact with the compound and in test 1, 2 and 4 the peak value is not reached within process time.

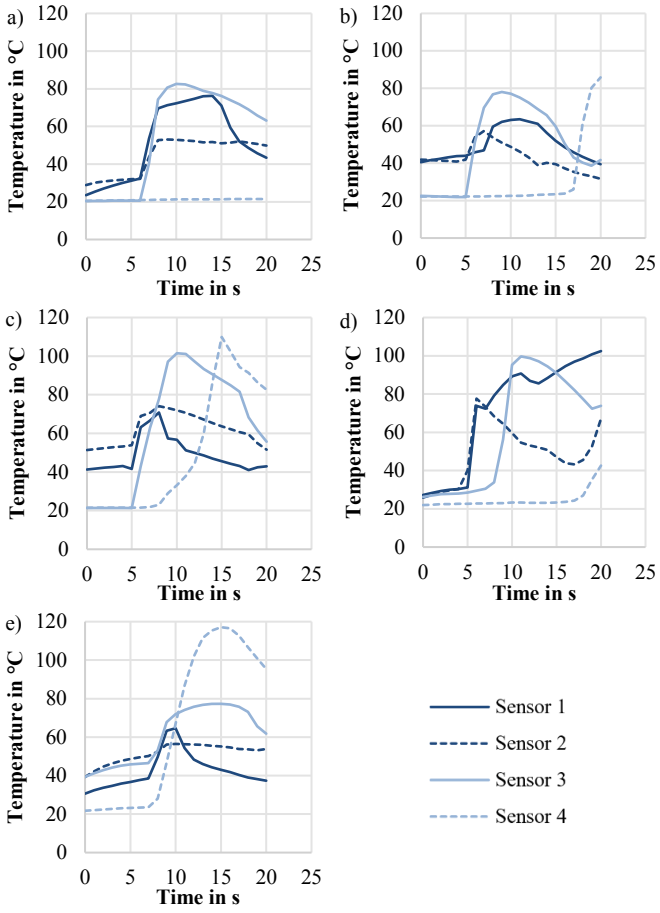


Fig. 8. Temperatures in test 1 to 5 at the sensor 1 to 4 are displayed in the diagrams a) to e)

With the presented experimental setup and the measurement technique, the forming process and the flow of the material can be observed. The measured temperature in the process indicates that the material flows from the inside of the compound to the outside while the material surface shows no relative movement to the tool. Experimental observations can be compared to the results of a finite element analysis. The results of the flow front progress depend strongly on the flow behaviour of the material, the initial location of the material and the correct execution of the tool movement.

## 4. Numerical model

In order to analyse the flow behaviour a numerical model is created in LS-DYNA and is displayed in Fig. 9. For simulation, only a section of the process has been selected in order to avoid long computation times.

The initial shape of the GMT is idealized as a rectangular geometry. Geometric deviations are neglected. The lower and the upper tool are modelled with help of rigid shell structures. The lower tool is fixed in space. In order to realise the particular complex forming motion of the upper tool the centre of gravity is artificially set outwards of the structure itself using the command *PART_INERTIA. Hereby, a rolling motion along a line 3 mm above the lower tool surface can be realised by the upper tool. The motion of the upper tool is depicted in Fig. 10. In the first phase, the upper tool translates downwards. In a

This is a resupply of March 2023 as the template used in the publication of the original article contained errors. The content of the article has remained unaffected.

second phase the rolling motion starts. This rolling motion is accomplished by overlapping a spatial as well as angular displacement boundary condition according to Figure 4. In order to obtain a time efficient model, mass scaling is applied to increase the effective time step size to 0.01 ms. Additionally, a time scaling procedure is performed in which the downwards motion is realised within 0.1 s and the subsequent rolling motion within 1 s.

It is assumed that the temperature decrease only takes place in a small boundary layer adjacent to the tool surface and that the temperature of the core has a temperature above the solidification temperature. The main deformation takes place in the core region. Consequently, the temperature decrease in the boundary layer has an insignificant influence on the overall forming behavior. Therefore, a quasi-isothermal approach for the simulation model is applied by using the averaged flow curve as input for the simulation model.

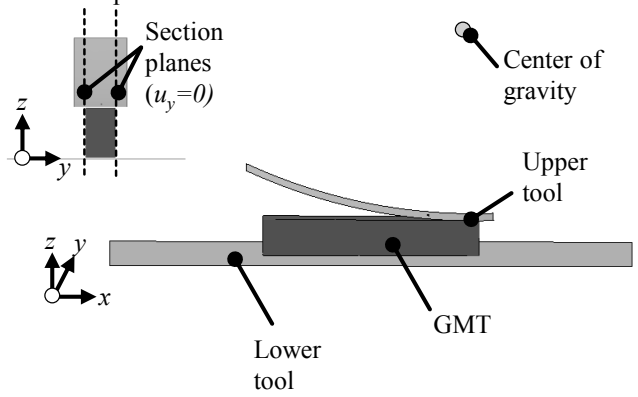


Fig. 9. Simulation model of the forming process

Due to the predominant low forming velocities in the forming process the strain rate dependencies are neglected and only the strain hardening effects are taken into account. The material model *MAT_PIECEWISE_LINEAR _PLASTICITY is applied. In order to account for strong mesh distortion of the GMT, an element-free Galerkin approach (EFG) in combination with remeshing has been selected for discretisation.

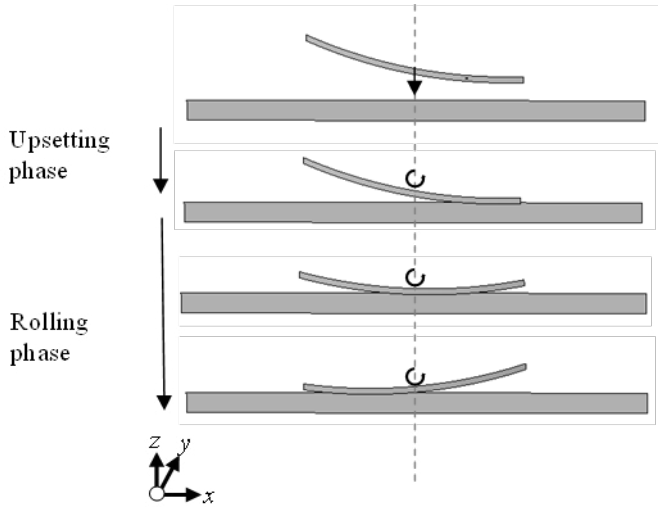


Fig. 10. Kinematic of the upper tool

## 5. Results and validation

The material flow predicted by the simulation model is shown in Fig. 11. In the upsetting phase, the GMT is squeezed sideways. During the subsequent rolling phase, the material continues to expand sideways until the forming phase is over.

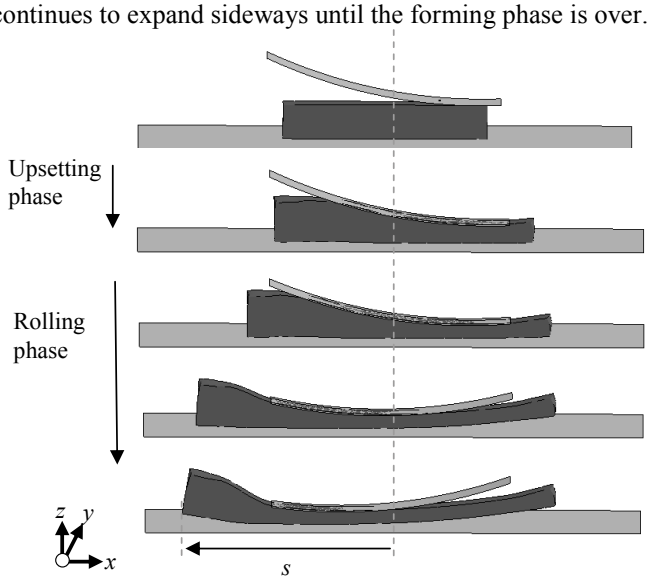


Fig. 11. Predicted material flow by numerical model

In order to compare the numerical results to the experimental results, the distance *s* which is measured from the tool middle to the outer right corner of the sample is plotted over time in Fig. 12. During the upsetting phase, the material is quickly squeezed to the sides, which results in a steep rise in the plot.

Followed by a less steep increase of the distance s caused by the continuous material flow during rolling phase. In the end of the process, the flow velocity decreases until the forming phase has completely terminated. This flow pattern was also observed in the experimental tests (see for instance Test 4). The quantitative deviations are in the range of the experimental results.

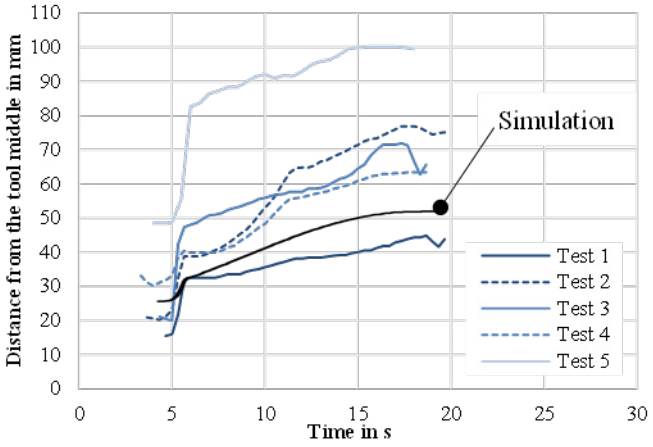


Fig. 12. Comparison of the experimentally and numerically predicted material flow

This is a resupply of March 2023 as the template used in the publication of the original article contained errors. The content of the article has remained unaffected.

## 6. Summary and conclusion

At first, a material characterisation of the used GMT has been carried out in order to describe the material behaviour. A set of experiments was conducted with a pressing and rolling movement. A six degree of freedom kinematics was used with an open die to observe the material flow in the process. The material flow depends on the insertion position and the initial shape of the GMT. Based on the material data a numerical model was set up in LS-DYNA, incorporating the particular difficult tool motion, consisting of an upsetting and a rolling phase. The predicted flow pattern shows good accordance with the experimental results for identical insertion positions. Minor deviations can be explained by the shape and amount of the material under the punch in the experiments.

## Acknowledgment

This work was funded by the Deutsche Forschungsgemeinschaft (DFG, German Research Foundation) – 318620418.

## References

[1] Radtke, A.: Steifigkeitsberechnung von diskontinuierlich faserverstärkten Thermoplasten auf der Basis von Faserorientierungs- und Faserlängenverteilungen (Fraunhofer IRB-Verl., Stuttgart, 2009)
[2] Behrens, B.-A., Hübner, S., Grbic, N., Micke-Camuz, M., Wehrhane, T., Neumann, A.: Forming and Joining of Carbon-Fiber-Reinforced Thermoplastics and Sheet Metal in One Step, 17th International Conference on Sheet Metal, SHEMET 2017, University of Palermo, Palermo, Italy; 10 April 2017 through 12 April 2017.
[3] Behrens, B.-A., Raatz, A., Hübner, S.,Bonk, C.,Bohne, F., Bruns, C., Micke-Camuz, M.: Automated Stamp Forming of Continuous Fiber Reinforced Thermoplastics for Complex Shell Geometries, 1st CIRP Conference on Composite Materials Parts Manufacturing, CIRP CCMPM 2017, Karlsruhe, Germany, 8 june through 9 june 2017.
[4] Kau, H.-T., Hagerman, E. M.: Experimental and analytical Procedures for Flow Dynamics of Sheet Molding Compound (SMC) in Compression Molding, Polymer Composites, Vol. 8, No. 3, 1987.
[5] Collyer, A. A., Clegg D.W.: Rheological Measurement, Springer Science+Business Media Dordrecht, 1998
[6] Engmann, J., Servais, C., Burbidge, A. S.: Squeeze flow theory and applications to rheometry: A review, Journal of Non-Newtonian Fluid Mechanics, 132, 2005, pp. 1-27
[7] Vahlund, C. F., Gebart, B. R.: Thermoplastic (GMT) in Large Tools and at High Closing Velocities, Intern. Polymer Processing XVII, 2002
[8] Kotsikos, G., Bland, J. H., Gibson, A. G: Rheological Characterization of Commercial Glass Mat Thermoplastics (GMTs) by Squeeze Flow Testing, Polymer Composites, Vol 20, 1999
[9] Behrens, B.-A.; Moritz, J.; Chugreev, A.; Bohne, F.; Schulze, H.: Finite Element Analysis for sheet metal reinforced hybrid structures produced via non-kinematical constraint manufacturing processes , 18th European Conference on Composite Materials, 24th - 28th june 2018, Athens, Greece
[10] Hesselbach, J., Behrens, B.-A., Dietrich, F., Rathmann, S., Poelmeyer, J.: Flexible forming with hexapods, Prod. Eng. Res. Devel., 2007, pp. 429-436

This is a resupply of March 2023 as the template used in the publication of the original article contained errors. The content of the article has remained unaffected.